Hierarchical ensembles: random fractals, flow fractals and the renormalisation group

1986 J. Phys. A: Math. Gen. 19 2395

(http://iopscience.iop.org/0305-4470/19/12/024)

J. Phys. A: Math. Gen. 19 (1986) 2395-2407. Printed in Great Britain

Hierarchical ensembles: random fractals, flow fractals and the renormalisation group

J R Melrose

Department of Chemistry, Royal Holloway and Bedford New College, Egham Hill, Egham, Surrey TW20 0EX, UK

Received 4 July 1985, in final form 6 November 1985

Abstract. Hierarchical ensembles possess exactly renormalisable partition functions. Examples studied in this work are iterative geometric constructions which at criticality give random self-similar fractals. The ensembles include novel non-self-similar constructions termed flow fractals here. The simple criticality of these ensembles is analysed and the self-similar fractals are found to be homogeneous. A multiple weight ensemble, the Ising snowflake, is introduced. The transfer matrix of fractals is defined via the renormalisation group. A discussion and interpretation is given of the eigenvalues of the transfer matrix fractals for the Ising snowflake.

1. Introduction

Naturally occurring fractals are members of a weighted ensemble of possible configurations or outcomes. Mandelbrot (1982) introduced random fractal constructions to aid the modelling of natural fractals. At the present time much work is being carried out on aggregation and percolation fractals generated by Monte Carlo techniques. However, explicit random constructions *á la* Mandelbrot have not received much attention. When considering ensembles it is natural to introduce a partition or generating function (Feller 1950). In this work partition functions are formed from a direct combination of the familiar iterative constructions with a simple renormalisation group (RG) scheme as introduced in Melrose (1985). Within this scheme the transfer matrices of fractals (Mandelbrot *et al* 1985, Aharony *et al* 1985) appear directly. At fixed points of the RG, self-similar constructions are found. In addition non-self-similar constructions (termed flow fractals here) are available by following renormalisation trajectories. By construction the ensembles considered below will be hierarchical, possessing a finite weight space RG. Section 2 gives the definition of a hierarchical ensemble and describes some one weight examples along with general rules of construction. Section 3 discusses the notion of geometric realisation and the choice of free coefficients in the examples. Section 4 discusses the critical behaviour and higher moments of the examples. Section 5 introduces a multiple weight example, the Ising snowflake. Section 6 defines the transfer matrices of fractals via familiar RG algebra and § 7 discusses the eigenvalues and eigenvectors of these matrices on the snowflake with particular attention paid to their geometric interpretation. Section 8 points out that hierarchical ensembles which are subsets of graphs of known Hamiltonian and geometric models can easily be found. Section 10 draws conclusions and presents the future outlook.

0305-4470/86/122395+13$02.50

2. Hierarchical ensembles: one weight examples

Below, configurations are generated by an iterative decoration. Let $Z_n(\bar{r})$ be the partition function for the ensemble of all configurations at the nth iteration. Then the ensemble is hierarchical if $Z_n(\bar{r})$ obeys the recursion

$$Z_n(\bar{r}) = Z_{n-1}(R(\bar{r}))K(\bar{r}) \tag{1}$$

where $\bar{r}$ is some finite set of q weights, $R(\bar{r})$ is a renormalisation recursion relation and q and $K(\bar{r})$ are independent of n. (The definition is a direct generalisation of the definition of hierarchical lattices (Griffiths and Kaufman 1982, 1984 and references therein) from lattices which naturally support hierarchical ensembles to hierarchical ensembles themselves.) The realisations in Euclidean space discussed below will all have $K(\bar{r}) = 1$; the author has not found Euclidean realisations with $K(\bar{r})$ non-unity. The simplest class has a single weight ($q = 1$), $\bar{r} = s$, $K(s) = 1$ and a polynomial recursion relation

$$s_k = R(s_{k-1}) = \sum_{L=p}^{m} a_{1L} s_{k-1}^{L}. \tag{2}$$

The partition function is given by the iterative substitution (1) and at the nth iteration one may introduce the coefficients a_{nL}:

$$Z_n(s) = \sum_{L=p^n}^{m^n} a_{nL} s^L = s_n = \sum_{L=p}^{m} a_{1L} s_{n-1}^{L}. \tag{3}$$

The examples discussed here are realisable (see § 3) as graphs in Euclidean space and will be formed by an iterative weighted decoration of edges or faces, etc, by some basic set of decorations (see below). The index L in (2) and (3) will stand for the number of edges or faces, etc, on a given configuration. Figures 1 and 2 respectively show basic sets of edge and face decorations used to construct ensembles in $d = 2$ space and $d = 3$ space. The hierarchical ensemble is specified by choosing the coefficients, a_{1L}, in (2); the description will be made in terms of edge decorations. A more general notation is necessary now: let b_{iL} be the chosen coefficient of the ith decoration of L edges in the basic set, so $a_{1L} = \Sigma_i b_{iL}$. The iteration of (2) is used to

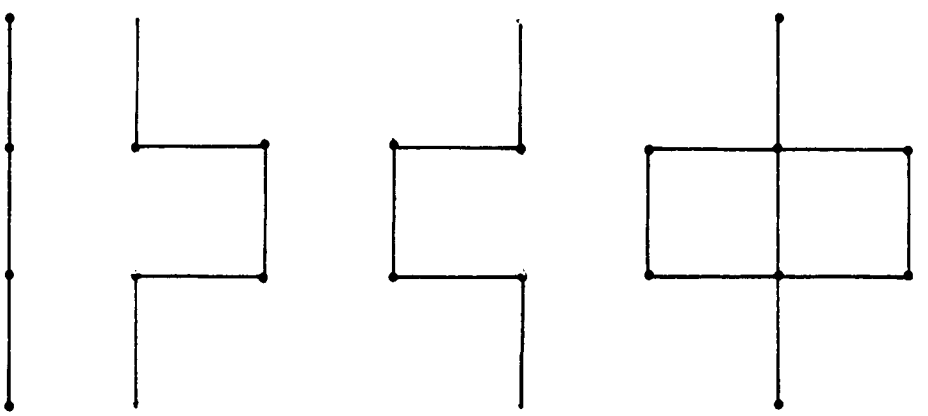

Figure 1. A basic set of decorations in the plane. These decorations are so chosen that they preserve the Eulerian nature of the generated graphs and hence could form the basis of an Ising ensemble in the sense of §§ 5 and 8.

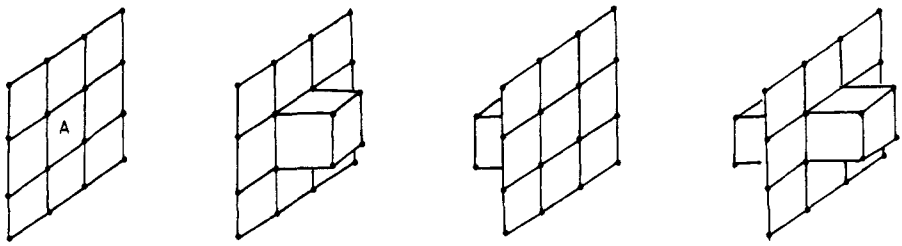

Figure 2. A basic set of decorations in 3-space. The middle face labelled A is included in the weighting only in the first and last decorations. These decorations could also form the basis of an Ising ensemble.

generate ensemble configurations at weight s as follows: if nth level configurations are required the recursion (2) is iterated n times: $s_0 = s$, $s_1 = R(s)$, $s_2 = R(R(s)), \ldots, s_n$. Then starting from a single edge an iterative decoration is carried out with, at the kth iteration, each edge in turn being decorated with the ith decoration of L edges, where i and L are chosen afresh for each edge with probability

$$b_{iL} s_{n-k}^{L} / Z_{n-k+1}(s). \tag{4}$$

The construction is simply the reverse of the renormalisation. With $b_{iL} > 0$ $\forall iL$ and $\mathrm{d}R(x)/\mathrm{d}x(x=0) = 0$, as henceforth assumed, the relations (2) have a single unstable fixed point: $s = s^* = s_1 = \ldots = s_n$. At s^* the construction described above is self-similar ((4) is independent of n) and typically will generate self-similar fractal configurations. Away from fixed points the non-self-similar configurations constructed by following some renormalisation trajectory, as described above, will be termed flow fractals.

3. Coefficients and realisation

The coefficients b_{iL} above are free to be chosen at will. For the one weight examples a simple equivalence exists between choices of b_{il}. Given some particular set of b_{il} specifying $R(s)$ and $Z_n(s)$ there exist equivalent ensembles defined on $\tilde{R}(\tilde{s}) = gR(\tilde{s}/g)$, where $g > 0$, which obey $\tilde{Z}_n(\tilde{s}) = gZ_n(\tilde{s}/g)$. Statistics for the equivalent ensembles (see below) are related by $\langle \widetilde{B(L)} \rangle_n(\tilde{s}) = \langle B(L) \rangle_n(\tilde{s}/g)$; $R(s)$ and $\tilde{R}(\tilde{s})$ have fixed points at s^* and gs^* respectively. If $g = 1/s^*$ then $s^* = 1$ and $\Sigma_{il} \tilde{b}_{il} = \Sigma_{il} (b_{il} s^{*L}/s^*) = 1$, then such coefficients are in this sense the normalised members of the equivalence class.

A particular class of coefficients of physical interest is now discussed. In general under the construction described above at each iteration all configurations with the same number, say L, of edges or faces, etc, are not equiprobable. However, physically interesting partition functions such as those of the Ising model and the generating functions for lattice animals and SAW (Stanley *et al* 1982) do have this property: all microstates with the same value for the state variables, in the examples L, are equiprobable. A choice of coefficients with this property is simply $b_{iL} = 1$ $\forall i, L$. For the examples of figures 1 and 2 equiprobable microstate (EPM) relations are respectively

$$s_k = s_{k-1}^3 + 2S_{k-1}^5 + s_{k-1}^9 \tag{5}$$

and

$$s_k = s_{k-1}^9 + 2s_{k-1}^{13} + s_{k-1}^{19}. \tag{6}$$

If one were to want to use such constructs as described here as simplified or pseudo-physical models, then for equilibrium problems choosing the EPM coefficients would seem desirable. However, under non-equilibrium or growth conditions equivalent microstates may not be equiprobable. Martin and Keefer (1985) also discuss the choice of coefficients on what are, in the terminology of the present work, one weight random fractal constructions.

The ensembles of interest here must satisfy both constraints of geometric realisation and hierarchical partition function. These constraints are now discussed couched in the terms of edge decorations in the plane.

The hierarchical constraint is that the decoration of a given configuration can be carried out independently on each basic shape (edges in figure 1), and that the renormalisation of the partition function factors on each basic shape. The geometric constraint is a question of what one chooses to allow with respect to the intersections and weighting of independent decorations. The set of decorations in figure 1 are chosen such that any protrusion is not allowed within a distance of the end vertices of the decoration equal to its own height. Hence under the decoration of different edges multiple edges are not generated. However the intersection of vertices under different decorations is allowed but in the weighting of the ensemble vertex sets are ignored. To this degree both geometric realisation and hierarchical construction are both satisfied. The geometric and hierarchical constraints are intimately bound together although formally independent of each other. Other hierarchical ensembles in the plane can be made by considering face decorations allowing the intersection of edges but just weighting on the number of faces. The beta model of turbulence (Benzi *et al* 1984 and references therein) is an example of this.

4. Expectations and critical behaviour

In the two examples configurations are specified by a single state variable L. Expectations of functions $B(L)$ over all nth level configurations are given by

$$\langle B(L)\rangle_n(s) = \sum_L B(L) a_{nL} s^L / Z_n(s). \tag{7}$$

In particular the expectation of the number of edges, faces, etc, $\langle L\rangle_n(s)$ is, using the iteration (1), given by

$$\langle L\rangle_n(s) = (s\, \mathrm{d}Z_n(s)/\mathrm{d}s)/Z_n(s) = \left(s \sum_{i=n-1}^{0} \lambda_1(i)\right) (Z_n(s))^{-1} \tag{8}$$

where $\lambda_1(k) = \mathrm{d}R(x)/\mathrm{d}x|_{x=s_k}$. With one weight, $s_n(s) = z_n(s)$. At a fixed point, s^*, $\langle L\rangle_n$ obeys the power law

$$\langle L\rangle_n(s^*) = \mathrm{d}s_n/\mathrm{d}s|_{s=s^*} = X_{1n}(s^*) = \lambda_{1^*}^N \tag{9}$$

where $\lambda_1^* = \mathrm{d}r(x)/\mathrm{d}x|_{x=s^*}$. The fixed point ensemble is associated with a fractal dimension D^* reflecting its statistical self-similarity:

$$D^* = \log(\lambda_1^*)/\log(b) \tag{10}$$

where it has been assumed that the embedding of the construction in Euclidean space endows it with a Euclidean metric such that an nth level configuration is of linear scale b^n for the two examples $b = 3$.

Numerically solving (5) and (6) gives $s^* = 0.6941$, $D^* = 1.3174$ and $s^* = 0.8892$, $D^* = 2.2740$ respectively.

At the sinks of the flow $s = 0$ and $s \to \infty$, the rule (4) with (2) generates configurations of dimension $D_0 = \log(p)/\log(b)$ and $D_\infty \log(m)/\log(b)$ respectively. For the example of figure 1 the $s = 0$ and $s \to \infty$ configurations are the 1D and a phi lattice (Given and Mandelbrot 1983).

On flow fractals the author introduces the definition of a flowing dimension

$$D(n, s) = \log(\langle L \rangle_n(s))/\log(b^n) \tag{11}$$

which being by definition a property of finite sets is strictly a function rather than a dimension. Figure 3 shows, for the example of figure 1, $D(n, s)$ for several s close to s^*. As $n \to \infty$ for $s < s^*$ and $s > s^*$, $D(n, s)$ approaches D_0 and D_∞ respectively. From (8) and (11) one finds

$$D(n, s) = \sum_{i=0}^{n} \log[s_{i-1}\lambda_1(i-1)/s_i]/n \log(b). \tag{12}$$

Using (2) reveals that $D(n, s)$ approaches D_0 and D_∞ as

$$\begin{aligned} D(n, s) &= D_0 + C(n, s)/n \log(b) \qquad \text{for } s < s^* \\ D(n, s) &= D_\infty - C'(n, s)/n \log(b) \qquad \text{for } s > s^* \end{aligned} \tag{13}$$

where $C(n, s)$ and $C'(n, s)$ are convergent series as $n \to \infty$, in practice converging rapidly with n. The $1/n$ approach to D_0 and D_∞ is seen in figure 3. With s close to s^*, $D(n, s)$ remains close to D^* before crossing over to (13) as C and C' converge. By analogy with other critical phenomena one may impose the concept of a correlation length $\mathscr{E} = [(s - s^*)/s^*]^{(-1/D^*)}$ and consider the recursion relation linearised at the

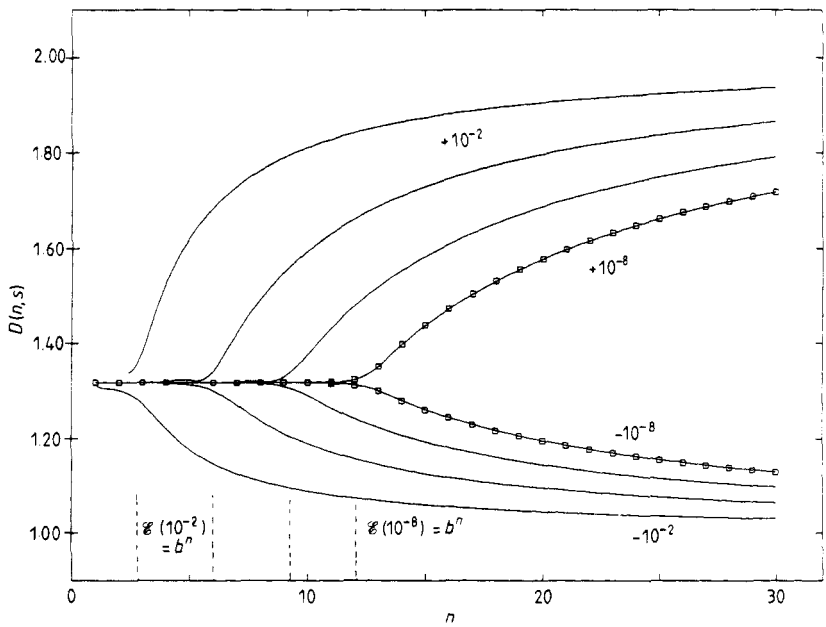

Figure 3. Flowing dimension against n for the example of figure 1 with $s - s^* = \mp 10^{-2}$, $\mp 10^{-4}$, $\mp 10^{-6}$ and $\mp 10^{-8}$.

fixed point for the mth iterate, $s' = s^* + \lambda_1^m(s - s^*)$. In the case $s < s^*$, informally allowing m to be non-integer, one finds m such that $s' = 0$ leading to $\mathscr{E}$ as given above with $\mathscr{E} = b^m$. Values for $\mathscr{E}$ are given in figure 3 and roughly correspond with the divergence of $D(n, s)$ from D^*.

An explicit expression for the second moment, $\langle L^2 \rangle$, of the self-similar ensembles at s^* is now found. Now, for general s,

$$\langle L^2 \rangle_n(s) = \langle L \rangle_n(s) + (s^2 \, \mathrm{d}^2 s_n(s)/\mathrm{d}s^2)/s_n(s) \tag{14}$$

where it is noted that $Z_n(s) = s_n(s)$. Let $X_{pk}(s) = \mathrm{d}^p s_k(y)/\mathrm{d}y^p\big|_{y=s}$ and $\lambda_p(s) = \mathrm{d}^p R(y)/\mathrm{d}y_p\big|_{y=s}$, with $\lambda_p(s^*)$ shortened to λ_p^* below. The fundamental recursion $s_n(s) = R(s_{n-1}(s))$ gives

$$X_{2n}(S^*) = \lambda_2^*(X_{1n-1}(s^*))^2 + \lambda_1^* X_{2n-1}(s^*). \tag{15}$$

Summing (15), substituting in the first moment (9) and substituting in (14) gives

$$\langle L^2 \rangle_n(s)^* = \lambda_1^{*N} + s^* \lambda_1^{*2n} \lambda_2^* (1 - \lambda_1^{*-n})/(\lambda_1^{*2} - \lambda_1^*). \tag{16}$$

Following Benzi *et al* (1984) a moment exponent ϕ_q is introduced via

$$\langle L^q \rangle_n(s^*) = k_{qn}(b^n)^{\phi_q}. \tag{17}$$

From (16) $\phi_2 = 2\log(\lambda_1^*)/\log(b) = 2D^*$ and $K_{2n} \to$ constant as $n \to \infty$. With increasing algebraic labour, recursion relations for higher derivatives may be found and summed using previous derivatives, and successive moments may be found using previous moments. The homogeneity, $\phi_p = pD^*$, found above for ϕ_p is suggested for all moments of the self-similar ensembles by the familiar linearised argument of the renormalisation group. As discussed in Melrose (1986) other random fractal constructions may not be homogeneous; in particular, if at each iteration all basic shapes are decorated with the same randomly chosen decoration then inhomogeneous fractals are constructed.

Fluctuations and moments away from fixed points are now discussed. Fluctuations in L, $f_n(s) = \langle L^2 \rangle_n - \langle L \rangle_n^2$ (the analogue of a specific heat), are found by iterating (14). In general one finds

$$f_n(s) = \sum_{i=0}^{n-1} a_i + \sum_{k=0}^{k-1} b_k \sum_{i=n-1}^{k+1} a_i \sum_{j=0}^{k-1} a_j^2 - \sum_{i=0}^{n-1} a_i^2 \tag{18}$$

where $a_i = s_i \lambda_1(s_i)/s_{i+1}$ and $b_i = s_i \lambda_2(s_i)/s_{i+1}$. For $s > s^*$ and $s < s^*$ one finds, using (2) and (18), that $f_n(s) = m^n k_n(s)$ and $f_n(s) = p^n k_n'(s)$ respectively, where k and k' are convergent series as $n \to \infty$ and identically $k_n'(0) = k_n(\infty) = 0$. With $p < b^D$ the density of fluctuations, $\lim_{n\to\infty} f_n(s)/b^{nd}$ is zero for $s < s^*$ and non-zero for $s > s^*$ only if $m = b^d$, its geometrical maximum. The usual scaling argument determines that the density of fluctuations, when non-zero, displays a singularity

$$\lim_{n\to\infty} f_n(s)/b^{nd} = (s - s^*)^{-2D^* + d} g[\ln(s - s^*)/\ln(\lambda_1^*)] \tag{19}$$

where $g(x) = g(1 + x)$; the periodic amplitude fluctuations are well known to be a possibility in models involving a discrete set of scale changes as b^n here (Derrida *et al* 1983 and references therein). In the direct geometric constructions here these amplitude fluctuations are much larger than those reported for physical models on hierarchical lattices by Derrida *et al* (1983). Figure 4 shows $f_n(s)/b^{nd}$ against $\ln(s - s^*)/\ln(\lambda_1^*)$ for the $n = 10$ finite hierarchy of figure 1. In the regime when $\mathscr{E}(s - s^*) < b^n$ the curve assumes the form (19) and when $(s - s^*)$ is such that $\mathscr{E}(s - s^*) > b^n$ the finite size is felt and the curve drops away to the fixed point value given by (16).

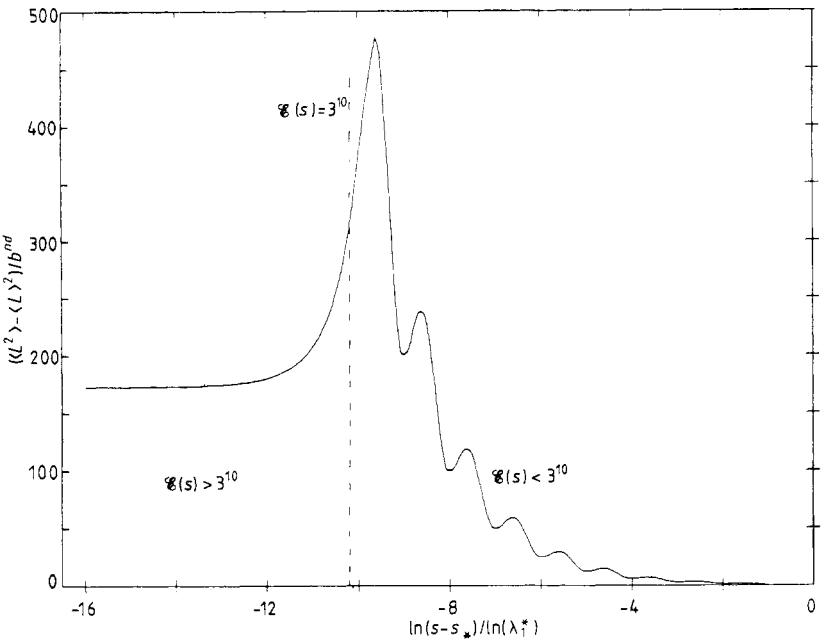

Figure 4. Fluctuations in L for the example of figure 1 with values of s close to s^* and $n = 10$.

5. The Ising snowflake

A multiple weight ensemble is now introduced. A set of basic shapes are now decorated with configurations made up of the same set. The Ising snowflake is based on the iterative decoration of boundaries separating 'black' and 'white' regions in the plane. Starting from a black triangle in a white background, at each step all black triangles are subdivided into nine and triangles with boundaries are decorated. Figure 5 shows the allowed decorations on a triangle with one boundary (cf the edge decorations of figure 1). Triangles with multiple boundaries may be decorated by all configurations formed as a direct product of the figure 5 decorations on the separate boundaries. The chosen decorations preserve the configurations as Eulerian graphs and hence the definition of black and white regions (a natural extension would be to relax this condition and to set up 'Potts' snowflakes). Weights r_0, r_1, r_2, r_3 are introduced conjugate to the basic shapes in the configurations: black triangles with zero to three black/white boundaries, all white triangles are given weight unity. An nth level configuration is given a weight

$$r_0^I r_1^J r_2^K r_3^L / Z_n(r_0, \ldots, r_3) \tag{20}$$

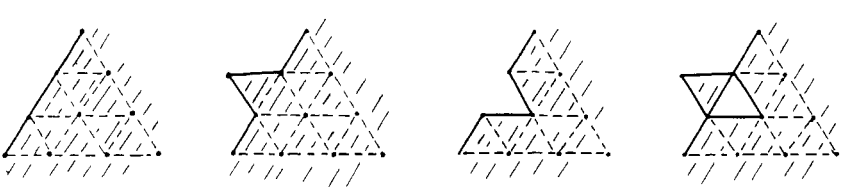

Figure 5. Decorations allowed on a triangle with one boundary. This shape is conjugate to r_1 and these decorations give the recursion relation $R_1(r)$ in (21) in the text. Black regions are shown shaded.

if it contains respectively I to L triangles with zero to three boundaries. The partition function, $Z_n(\bar{r})$, obeys the hierarchical condition (1) and the recursion relations can be found by subdividing and decorating black triangles with zero to three boundaries. Straightforward enumeration (see figure 5 for r_1') yields for the EPM choice of coefficients:

$$\begin{aligned}
r_0' &= R_0(\bar{r}) = r_0^9 \\
r_1' &= R_1(\bar{r}) = r_0^4 r_1^2[r_0^2(r_1 + r_0 r_2) + r_1^2(1 + r_3)] \\
r_2' &= R_2(\bar{r}) = r_0 r_1^2 r_2[r_0^3(r_1 + r_0 r_2)^2 + 2r_0 r_1^2(r_1 + r_0 r_2)(1 + r_3) + r_2 r_1^2(1 + r_3)^2] \\
r_3' &= R_3(\bar{r}) = r_2^3[r_0^3(r_1 + r_0 r_2)^3 + 2r_0 r_1^2(r_1 + r_0 r_2)^2(1 + r_3) \\
&\qquad + 3r_1^2 r_2(r_1 + r_0 r_2)(1 + r_3)^2 + r_2^3(1 + r_3)^3].
\end{aligned} \tag{21}$$

The notation r_{ik} will be used to denote the ith field in the set $\bar{r}_k$ given by the kth iterate of (21) from some initial set of fields $\bar{r}_0$ (where unambiguous, r_{i0} will be shortened to r_i below). As described in § 1 configurations within the nth level ensemble can be generated by following the reverse of the flow of (21); at the mth decoration a pth type of black triangle is decorated according to the weight

$$r_{0n-m}^I r_{1n-m}^J r_{2n-m}^K r_{3n-m}^L / r_{pn-m+1}. \tag{22}$$

The decoration is assumed to start from a black triangle with three boundaries conjugate to r_3; hence $Z_n(r_{00}r_{10}r_{20}r_{30}) = r_{3n}(r_{00}r_{10}r_{20}r_{30})$.

Note that the above construction is in general not based on independent boundary decorations (e.g. figure 1), but rather independent triangle decorations; the weight r_2 in (21) couples decorations of different boundaries of the same triangle. Figure 6 shows some of the decorations of a two bounded triangle. The first of these, for example, gives a term $r_0 r_1^4 r_2^2$ to the relation $R_2(\bar{r})$. The recursion relations have the invariant subspaces $(r_0 = 1)$, $(r_0 = 1,\ r_2 = r_3 = 0)$ and $(r_0 = 1,\ r_1 = s,\ r_2 = s^2,\ r_3 = s^3)$. In the last of these subspaces, the boundary subspace, configurations are weighted just on the number of black/white boundaries and decorations do factor on separate boundaries of the same triangle. The ensembles in this subspace can be constructed via independent boundary decorations. This simplicity will allow an understanding of the geometry of this subspace to be given in § 7. Flows within the boundary subspace are given by the recursion relation

$$s' = s^3 + 2s^4 + s^7 \tag{23}$$

cf equations (5) and (6). An unstable fixed point of (23) is found at $s^* = 0.639\,404$.

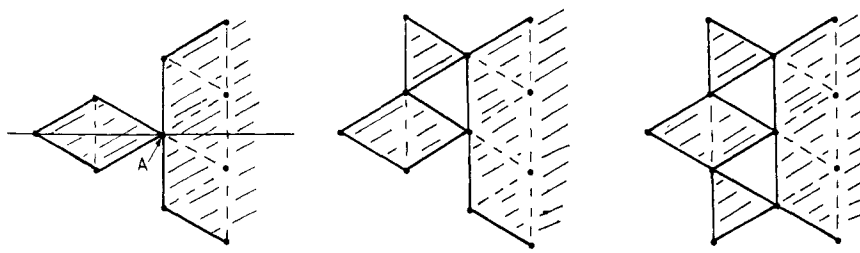

Figure 6. The decorations of a two bounded triangle which include internal intersections at site A on a line, indicated in the first decoration, through one apex of the triangle.

The full space contains, in various weighting limits, a number of deterministic fractals and regular random fractals (Martin and Keefer 1985). A second unstable fixed point is found on the r_1 axis in the ($r_0 = 1$, $r_2 = r_3 = 0$) subspace. Restricting the decorations to be those formed from just the first three configurations of figure 5 constitutes a subensemble as none of these decorations introduce triangles with three boundaries. The recursion relations (21) separate into terms with and without powers of r_3 and the relations for the subensemble are those terms without r_3.

6. Expectations and the transfer matrix

Expectations formulated as derivatives of the partition function can be found by familiar RG matrix algebra. Let some quantity of interest, Q_x, be associated with a conjugate field x via $r_{i0} = f_i(x, \theta)$, with θ some other set of fields in the problem. Then if

$$\langle Q_x \rangle_n = [x \, \mathrm{d}Z_n(\bar{r}(x))/\mathrm{d}x]/Z_n(\bar{r}(x)) \tag{24}$$

and using the chain rule and the hierarchical property (1), one finds after some rearrangement

$$\langle Q_x \rangle_n = \boldsymbol{V}_n \prod_{m=1}^{n} T_m \boldsymbol{V}_0 \tag{25}$$

where the ith element of the vector $\boldsymbol{V}_n$ obeys $(\boldsymbol{V}_n)_i = \delta_{ik}$, with k the index of the basic shape used to initiate decoration, $(\boldsymbol{V}_0)_i = x \, \mathrm{d}r_{i0}/\mathrm{d}x$ and T_m is a set of $q * q$ matrices:

$$(T_m)_{ij} = (r_{jm-1}(\mathrm{d}R_i(\bar{r})/\mathrm{d}r_j | \bar{r} = \bar{r}_{m-1})/r_{im}. \tag{26}$$

$(T_m)_{ij}$ is the expected number of jth type basic shapes introduced on an ith type basic shape at the $(n-m+1)$th decoration. T_m is the natural generalisation both to an ensemble and flow fractals of the transfer matrix of fractals introduced recently by Mandelbrot *et al* (1985). Note the RG gives the transpose of the matrix defined by Mandelbrot *et al* and attention is focused on the right eigenvectors as the quantities whose expectation is to be found. For the snowflake a choice of fields

$$r_{00} = r \qquad r_{10} = rs \qquad r_{20} = rs^2 \qquad r_{30} = rs^3 \tag{27}$$

has r conjugate to the black area and s conjugate to the boundary length. One finds that the expectation of the area is given by (25) with $V_0 = (1, 1, 1, 1)$ and of the boundary by $V_0 = (0, 1, 2, 3)$.

7. Eigenvalues of the snowflake TMF

Following Mandelbrot *et al* (1985) it is possible to interpret eigenvalues of the TMF as being associated with dimensions and expectations of subsets of the full configurations. The TMF of the snowflake are given by substituting (21) in (26) and are a set of matrices parametrised by (r_0-r_3). Throughout the discussion below, the boundary subspace, (27) with $r = 1$, will be denoted by $\{B\}$. As will be seen the factorisation (see § 5) in this subspace allows explicit interpretation of all the eigenvalues of the subspace TMF.

From (21) one sees that $\lambda_a = 9$ is an eigenvalue of all the TMF. This eigenvalue is taken to give the dimension of the black area, $D_a = \log(9)/\log(3) = 2\ \forall (r_0 - r_3)$. The area vector (1, 1, 1, 1), however, is only the corresponding eigenvector for the TMF in $\{B\}$; it is proved that $\Sigma_j T_{ij} = 9\ \forall \{B\}$ using the fact that the set of decorations on each shape are such that for each of weight s^L with area $9+\Delta$ there is another also of weight s^L but with area $9-\Delta$. This eigenvector (1, 1, 1, 1) is lost in $\{B\}$ by breaking this symmetry. That in general (1, 1, 1, 1) is not an eigenvector simply implies that away from $\{B\}$ the black area is not self-similar, although as n increases it rapidly approaches 9^n. The second largest eigenvalue, λ_b, is found numerically to be greater than 3 and is taken to be associated with the length of the black/white boundary. The variation of λ_b in $\{B\}$ is as described for the ensembles of figures 1 and 2 in § 4. The boundary vector (0, 1, 2, 3) is the corresponding eigenvector only for the TMF in $\{B\}$; this can be proved using the factorisation in $\{B\}$ of decorations into independent boundary decorations. In general expectations of vectors of the form (x, y, z, w) are dominated by the eigenvalue λ_a whilst those of the form $(0, x, y, z)$ are dominated by the eigenvalues $\lambda_b(r_0 - r_3)$.

The other two eigenvalues of the TMF are less easily understood. However, in $\{B\}$ interpretations of these can be found. In $\{B\}$ expectations of quantities, $\langle Q \rangle_p$, which are a sum over the p separate boundary decorations on a p bounded shape, $Q_p = q_1 + \ldots + q_p$, obey

$$\langle Q \rangle_p = p \langle Q \rangle_1. \tag{28}$$

Examples of such are the expectation, $T_{p3}(\{B\})$, of the number of three bounded triangles over the decorations of a pth bounded shape and $T_{i1}(\{B\}) - 2T_{i2}(\{B\})$, the expectation of the number of boundaries other than those on three bounded triangles over the decorations of a pth bounded shape. Using (28) one finds the ratios of these expectations are constant over p:

$$T_{13}/(T_{11} + 2T_{12}) = T_{23}/(T_{21} + 2T_{22}) = T_{33}/(T_{31} + 2T_{32}) = k(s) \tag{29}$$

where $k(s) = s^7/(3s^3 + 8s^4 + 4s^7)$. From (29), the fourth column of the TMF in $\{B\}$ is not linearly independent and the TMF are singular with corresponding eigenvector $(0, x, 2x, -y)$ with $x/y = k(s)$.

Using the identity $\mathrm{Tr}\ T = \Sigma_i \lambda_i$ one finds the fourth eigenvalue, λ_I (I for intersection), in $\{B\}$ is given by

$$9 + T_{11} + T_{22} + T_{33} = 9 + (T_{11} + 2T_{12} + 3T_{13}) + 0 + \lambda_I \tag{30}$$

and using $T_{33} = 3T_{13}$ gives

$$\lambda_I = T_{22}(\{B\}) - 2T_{12}(\{B\}) = 1 + (s^8 + 2s^{11} + s^{14})/s'^2. \tag{31}$$

One finds that λ_I is $1 + \Sigma_I$, where Σ_I is a sum over the weights of the decorations of a two bounded triangle which have internal intersections. These are shown in figure 6. Interpretation is easy: $\log(\lambda_I)/\log(b)$ is the fractal dimension of the set of vertices lying at the intersection of independent boundary decorations and on a line bisecting the apex of the original basic shape (see figure 6). At the mth decoration iteration the number of such intersections introduced per such intersection is just $\lambda_I(s_{n-m})$; the 1 in λ_I counts the original intersection.

In summary a zero eigenvalue is found in $\{B\}$ due to the presence of two independent quantities whose expectations are sums over independent boundary decorations (the 'direct product' nature of the decorations introducing three bounded triangles is evident

in figure 5). An intersection eigenvalue gives the fractal dimension of a special cut set of the configurations.

8. Subsets of known models

The low temperature graphs for an Ising model on a hexagonal lattice (Domb and Green 1973) are all the Eulerian graphs on its dual lattice, the triangular lattice. The configurations of the snowflake ensemble are a subset of these graphs, each black(white) triangle corresponding to an up(down) spin and each black/white boundary cutting an unsatisfied bond on the hexagonal lattice. After removal of a constant one makes the following identification between the subspace (27) and the usual Ising weighting:

$$s = \exp(-2J) \qquad r = \exp(-2h) \tag{32}$$

where J and h are the reduced Ising coupling and external field respectively. Although the snowflake ensemble is such a subset possessing a phase transition it bears little resemblance to the full Ising model. With polynomial recursion relations only a stable (high temperature) fixed point at $J = 0$ cannot be found. The phase transition in the snowflake involves just the boundary set. Fixed points of the snowflake have more than the two relevant eigenvalues expected for the Ising model. The snowflake is a crude droplet model (Fisher 1967) and can be improved somewhat in this respect by allowing more excluded volume effects: for example, by adding internal white triangles where possible on the original set of decorations. The boundary subspace would be lost but the possibility of phase transitions involving both boundary and area would be opened up. However, to find other than polynomial recursion relations would require the constructions to be part of a wider scheme of real space renormalisation approximations. Recursion relations for Ising models on hierarchical lattices are rational algebraic expressions (Melrose 1983).

Geometric models such as SAW and lattice animals do have polynomial recursion relations (Stanley *et al* 1982) and it is easy to find hierarchical subsets of these ensembles. (An example is given in Melrose (1985).) The relationship of such ensembles to the full ensembles is an interesting question.

9. Deterministic and regular random fractals

Deterministic fractals (one decoration per basic shape) and regular random fractals (multiple decorations per basic shape but each having the same numbers of each subshape (Martin and Keefer 1985)) can both be associated trivially with one-term polynomial recursion relations of the form, for a p sided shape,

$$r_i' = m_i r_1^{i_1} \ldots r_p^{i_p} \tag{33}$$

with $m_i = 1$ (integer) for deterministic (regular random) fractals. Expectations from (33) are constant throughout the weight space and the RG flow is meaningless; i_j is the ijth element of the transpose of the TMF of Mandelbrot *et al* (1985). Unlike the examples in the present work the random TMF of Mandelbrot *et al* (1985) are a weighted sum of deterministic TMF.

10. Discussion and conclusions

The purpose of this work has been to introduce the formalism required to realise hierarchical ensembles in Euclidean space. By combining the familiar iterative constructions of Mandelbrot with renormalisation algebra, the generating functions for ensembles containing random fractals at phase transitions were open to analysis. Introducing the RG and the full ensemble brought about the existence of flow fractal constructions. The field of critical phenomena is rife with crossover effects which beg the existence of flow fractals. Other physical phenomena may show a slow approach to an asymptotic dimension: molecular paths in simulations have been argued recently to show such behaviour (Powles and Quirke 1984, Powles 1985, Kalia *et al* 1985). The simple critical behaviour of such ensembles and associated anomalies, such as periodic critical amplitudes, was discussed. A multiple weight ensemble, the Ising snowflake, was described and the transfer matrix of fractals, introduced recently by Mandelbrot *et al* (1985), arose naturally in the multiple weight scheme. Explicit geometric interpretation of the eigenvalues of the snowflake TMF was given. Mandelbrot *et al* (1985) found that the TMF of all finitely ramified deterministic constructions were singular here; a singular TMF was associated with a subtle direct product nature of the random construction in a particular weight subspace. One eigenvalue was shown to be associated with a special cut set of the construction; this is interesting in the context of interpreting eigenvalues of TMF in less explicit problems such as the percolation cluster studies of Aharony *et al* (1985).

The hierarchical ensembles introduced above do, by definition, constitute solvable ensembles with phase transitions in any Euclidean space. It was noted that hierarchical subsets of known models may easily be found and this may be of use in statistical mechanics. However, the ensembles are constrained on all scales and show non-universal behaviour; one finds for example that a Monte Carlo algorithm to sample the configuration space would need to be able to flip and alter configurations on all scales.

As random fractal constructions, use may be made of these ensembles as models of rough surfaces. However, one might then want to place physical models on the configurations but with the examples in this work the intersection of vertices under independent decorations makes this problematical: one may either treat the configurations as connected or disconnected at such vertices and only in the latter case can the renormalisation solve models placed on the configurations. However Monte Carlo investigations of diffusion onto, off and around generated configurations are feasible.

Acknowledgments

The author would like to thank the SERC for a postdoctoral scholarship. The author dedicates this paper to the memory of his late father, Dr D R Melrose, and his life of research work in veterinary science.

References

Aharony A, Gefen Y, Kapitulnik A and Murat M 1985 *Phys. Rev.* B **31** 4721
Benzi R, Paladin G, Parisi G and Vulpiani A 1984 *J. Phys. A: Math. Gen.* **17** 3521

Derrida B, Eckmann J P and Erzan A 1983 *J. Phys. A: Math. Gen.* **16** 893
Domb C and Green M S 1973 *Phase Transitions and Critical Phenomena* vol 3, ed C Domb and M S Green (New York: Academic)
Feller W 1950 *Introduction to Probability Theory and its Applications* vol 1 (New York: Wiley)
Fisher M E 1967 *Rep. Prog. Phys.* **30** 616
Given J A and Mandelbrot B 1983 *J. Phys. A: Math. Gen.* **16** L565
Griffiths R B and Kaufman M 1982 *Phys. Rev.* B **26** 502
—— 1984 *Phys. Rev.* B **30** 244
Kalia R K, de Leeuw S W and Vashishta P V 1985 *J. Phys. C: Solid State Phys.* **18** L905
Mandelbrot B B 1982 *The Fractal Geometry of Nature* (San Francisco: Freeman)
Mendelbrot B B, Gefen Y, Aharony A and Peyiere J 1985 *J. Phys. A: Math. Gen.* **18** 335
Martin J E and Keefer K D 1985 *J. Phys. A: Math. Gen.* **18** L625
Melrose J R 1983 *J. Phys. A: Math. Gen.* **16** 3077
—— 1985 *Conf. Proc. 6th Trieste Symp. on Fractals* (Amsterdam: North-Holland)
—— 1986 *J. Phys. A: Math. Gen.* **19** 821
Powles J G 1985 *Phys. Lett.* **107A** 403
Powles J G and Quirke N 1984 *Phys. Rev. Lett.* **52** 1571
Stanley H E, Reynolds P and Klein M 1982 *Real Space Renormalisation* ed T W Burkhardt and J M J van Leeuwen (Berlin: Springer) p 169